

Robust superconductivity with large upper critical field in Nb₂PdS₅

Rajveer Jha, Brajesh Tiwari, Poonam Rani, Hari Kishan, and V. P. S. Awana

Citation: *Journal of Applied Physics* **115**, 213903 (2014); doi: 10.1063/1.4881278

View online: <http://dx.doi.org/10.1063/1.4881278>

View Table of Contents: <http://scitation.aip.org/content/aip/journal/jap/115/21?ver=pdfcov>

Published by the [AIP Publishing](#)

Articles you may be interested in

[Superconductivity in BiS₂ based Bi₄O₄S₃ novel compound](#)

AIP Conf. Proc. **1512**, 1104 (2013); 10.1063/1.4791432

[Interstitial doping induced superconductivity at 15.3K in Nb₅Ge₃ compound](#)

J. Appl. Phys. **111**, 123912 (2012); 10.1063/1.4730611

[Angular dependence of pinning potential, upper critical field, and irreversibility field in underdoped BaFe_{1.9}Co_{0.1}As₂ single crystal](#)

Appl. Phys. Lett. **100**, 102601 (2012); 10.1063/1.3692582

[Superconductivity In Y₂Pd\(Ge_{1-x}Si_x\)₃ \(x = 01\)](#)

AIP Conf. Proc. **850**, 649 (2006); 10.1063/1.2354877

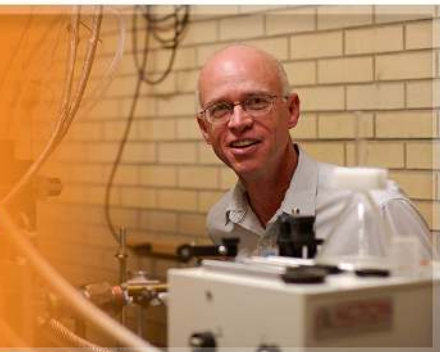
[Superconducting Transition Temperature of \(Nb_{1-x}Zr_x\)_{0.8}B₂](#)

AIP Conf. Proc. **850**, 639 (2006); 10.1063/1.2354872

The logo for Applied Physics Letters (AIP) is displayed. It features the letters 'AIP' in a large, white, sans-serif font on the left, followed by a vertical line and the words 'Applied Physics Letters' in a smaller, white, sans-serif font on the right. The background is a dark orange with a subtle, swirling pattern.

AIP | Applied Physics
Letters

is pleased to announce **Reuben Collins**
as its new Editor-in-Chief



Robust superconductivity with large upper critical field in Nb₂PdS₅

Rajveer Jha, Brajesh Tiwari, Poonam Rani, Hari Kishan, and V. P. S. Awana^{a)}
*Quantum Phenomena and Applications Division, National Physical Laboratory (CSIR),
 Dr. K. S. Krishnan Road, New Delhi-110012, India*

(Received 25 April 2014; accepted 21 May 2014; published online 3 June 2014)

We report synthesis, structural details, and complete superconducting characterization of very recently discovered [Q. Zhang, *Sci. Rep.* **3**, 1446 (2013)] Nb₂PdS₅ new superconductor. The synthesized compound is crystallized in monoclinic structure with *C2/m* (#12) space group. Bulk superconductivity is seen in both *ac/dc* magnetic susceptibility and electrical resistivity measurements with superconducting transition temperature (T_c) at 6 K. The upper critical field (H_{c2}) being estimated from high field magneto-transport [$\rho(T)H$] measurements is above 240 kOe. The estimated $H_{c2}(0)$ is clearly above the Pauli paramagnetic limit of $\sim 1.84T_c$. Heat capacity (C_p) measurements show clear transition with well defined peak at T_c , but with lower jump than as expected for a Bardeen–Cooper–Schrieffer type superconductor. The Sommerfeld constant (γ) and Debye temperature (Θ_D) as determined from low temperature fitting of $C_p(T)$ data are 32 mJ/mole·K² and 263 K, respectively. Hall coefficients and resistivity in conjugation with electronic heat capacity indicates multiple gap superconductivity signatures in Nb₂PdS₅. We also studied the impact of hydrostatic pressure (0–1.97 Gpa) on superconductivity of Nb₂PdS₅ and found nearly no change in T_c for the given pressure range. © 2014 AIP Publishing LLC. [<http://dx.doi.org/10.1063/1.4881278>]

INTRODUCTION

Very recently discovered superconductivity in layered Nb₂PdS₅ along with superconductivity of Fe based oxypnictides i.e., REFeAsO/F has attracted huge attention of scientific community.^{1,2} In fact, seemingly it was like second revolution after the invention of high T_c cuprates superconductivity way back in 1986 (Ref. 3) Though other superconductors like famous MgB₂ keep on adding,⁴ but it is only after the Fe pnictides that search for new superconductors is sparked once again. Besides several Fe pnictide^{5,6} and chalcogenide^{7,8} families, some other similar structure compounds viz. the BiS₂ based^{9–11} ones are added more recently. When looking for new superconductors, one aspires for best superconducting properties, such as higher critical temperature (T_c) and upper critical field (H_{c2}). In general, it is a feast for a scientist to discover a higher T_c and H_{c2} superconductor. Both parameters are important for practical applications of a superconductor. Besides the higher T_c , which helps in reducing the operating temperature cost, the upper critical field warrants the robustness of the superconductor against magnetic field. In this direction, the recently discovered Nb₂PdS₅ superconductor,^{1,12} though possess comparatively lower T_c of around 6 K only, but the same is quite robust against magnetic field.

The robustness of superconductivity does mean here that superconductivity is least affected by the applied magnetic field. Generally speaking, the decrease of T_c with applied magnetic field, i.e., dT_c/dH determines the upper critical field in a simple single band scenario.¹³ In a type II superconductor, the upper critical field can be enhanced by both intrinsically^{6,14} and extrinsically.¹⁵ Intrinsically, the same happens

in multi band systems having complicated electronic^{6,14} and extrinsically by pinning the vortices in their mixed state.¹⁵ The recently discovered superconductor, i.e., Nb₂PdS₅ seems to be both intrinsically robust as well as pinned by inherent defects, etc. It is noteworthy here that Nb is the most popular superconductor being used till date in superconductor industry having varying superconducting transition temperature (T_c) values in various metal or alloy forms from 9 K(Nb), 11.5 K(NbC), 16 K(NbN), 19 K(Nb₃Sn) to 23 K(Nb₃Ge).^{16–20}

The recent compound, i.e., Nb₂PdS₅ somehow reminds not only the importance of Nb being the part of various superconductors in past,^{16–20} but also the presence of S in its layered structure calls for the attention of famous high upper critical field S containing Chevrel phase compounds.²¹ Keeping in view the importance of Nb and the utility of S in new layered structure of the recent compound Nb₂PdS₅, we present here an easy and clear route of synthesis of this new superconductor. Further full superconducting characterization in terms of high field (140 kOe) and low temperature (down to 2 K), electrical, magnetic, and thermal characterizations are presented in current communication.

EXPERIMENT

Polycrystalline bulk Nb₂PdS₅ is synthesized via solid state reaction route by quartz vacuum encapsulation technique at 850 °C. The high purity (4N) ingredients, i.e., Nb, Pd, and S are weighed in stoichiometric ratio and mixed thoroughly in a glove box in Ar atmosphere. The mixed powder is pelletized, sealed in an evacuated quartz tube, and put immediately in box furnace. The sample is heated to 850 °C with heating rate of 3 min and hold at same temperature for 24 h. Subsequently, the furnace is switched off and allowed to cool to room temperature over a span of 6 h. Thus, obtained sample is once again pulverized, pelletized, sealed in encapsulated

^{a)} Author to whom correspondence should be addressed. E-mail: awana@mail.nplindia.org. Telephone +91-11-45609357, Fax: +91-11-45609310

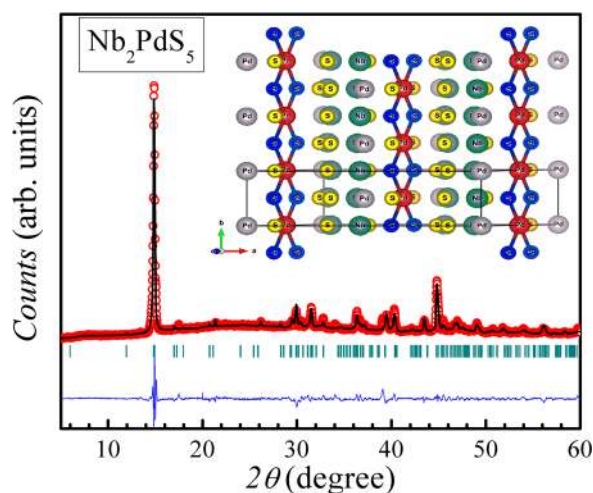


FIG. 1. Rietveld refined Room temperature XRD patterns of Nb_2PdS_5 , the unit cell of the compound is shown in inset.

quartz tube, heated at same temperature for another 24 h, and furnace cooled to room temperature. The room temperature X-ray diffraction (XRD) patterns are taken after each heat treatment on Rigaku XRD machine. The electrical, magnetic, and thermal characterization is done with help of Quantum Design (QD) Physical Property Measurement System (PPMS)—140 kOe down to 2 K. Hydrostatic pressures are generated by a BeCu/NiCrAl clamped piston-cylinder cell using HPC-33, an addition to PPMS QD, to study the pressure effect on Nb_2PdS_5 . The pressure at low temperature was calibrated from the superconducting transition temperature of Pb. The sample is immersed in a fluid pressure transmitting medium of Fluorinert in a Teflon cell. Annealed Pt wires were affixed to gold-sputtered contact surfaces on each sample with silver epoxy in a standard four-wire configuration.

RESULTS AND DISCUSSION

The synthesized Nb_2PdS_5 sample is gray in color. The room temperature fitted and observed XRD pattern for the synthesized Nb_2PdS_5 along with its unit cell is shown in Figure 1. Nb_2PdS_5 crystallizes in Centro-symmetric structure within space group $C2/m$ (#12). There are two formula units in each unit cell comprising two sites each for Nb (Nb1, Nb2) and Pd (Pd1, Pd2) along with five S sites (S1, S2, S3, S4, S5). The schematic sketch of the unit cell is shown in inset of Fig. 1. Details of Wyckoff positions, site symmetry, and fractional occupancies being obtained from Rietveld fitting of the experimental XRD data are given in Table I. The lattice parameters are $a = 12.134(2)\text{\AA}$, $b = 3.277(1)\text{\AA}$, $c = 15.023(3)\text{\AA}$, with $\alpha = 90^\circ$, $\beta = 103.23^\circ(1)$ and $\gamma = 90^\circ$. Structural detail results are in general agreement with another recently discovered similar superconducting compound Ta_2PdS_5 .²²

In a very recent electronic structure determination theoretical article,²³ slightly different configuration is used, i.e., high conductivity direction is labeled along c -axis instead of usual b -axis.^{1,22} In fact due to anisotropic nature of the conductivity in different Pd-S chains/sheets, the superconducting upper critical field is highly directional dependent in

TABLE I. Rietveld refined Wyckoff positions and fractional occupancies of the atoms in Nb_2PdS_5 .

Atom	x	y	z	site	Fractional occupancy
Nb1	0.0759(5)	0.5000	0.179(4)	4i	1
Nb2	0.1528(8)	0.0000	0.3783(2)	4i	1
Pd1	0.0000	0.0000	0.0000	2a	1/2
Pd2	0.0000	0.0000	0.5000	2c	1/2
S1	0.3503(6)	0.0000	0.4890(1)	4i	1
S2	0.2537(4)	0.5000	0.2950(6)	4i	1
S3	0.1753(6)	0.0000	0.0977(8)	4i	1
S4	0.4230(3)	0.5000	0.1321(4)	4i	1
S5	0.4904(7)	0.0000	0.3234(6)	4i	1

these compounds.^{1,22,23} In a more recent communication,²⁴ the $\text{Nb}_2\text{Pd}_x\text{S}_{5-y}$ fiber exhibited slightly modified superconducting parameters including higher T_c of 7.14 K. The role of off stoichiometry and directional alignment could lead to changed superconducting characteristics. Here, we stick to stoichiometric Nb_2PdS_5 bulk polycrystalline compound to minimize the complications.

AC susceptibility versus temperature $\chi(T)$ behavior of the Nb_2PdS_5 sample is depicted in Figure 2. AC susceptibility measurements are done at 33 Hz and 10 Oe AC drive field. DC applied field is kept zero to check the superconducting transition temperature (T_c). Both the real (χ') and imaginary (χ'') part of ac susceptibility are measured. Real part (χ') susceptibility shows transition to diamagnetism at around 5.8 K, confirming bulk superconductivity. The imaginary part on the other hand exhibits a single sharp peak in positive susceptibility at around the same temperature. Presence of single sharp peak in χ'' is reminiscent of better superconducting grains coupling in studied Nb_2PdS_5 superconductor. We also measured the AC susceptibility of the compound in applied dc fields of up to 120 kOe. The plot of real part (χ') of ac susceptibility with applied field is depicted in inset of Figure 2. The temperature is fixed at 3 K, i.e., well below the superconducting transition temperature

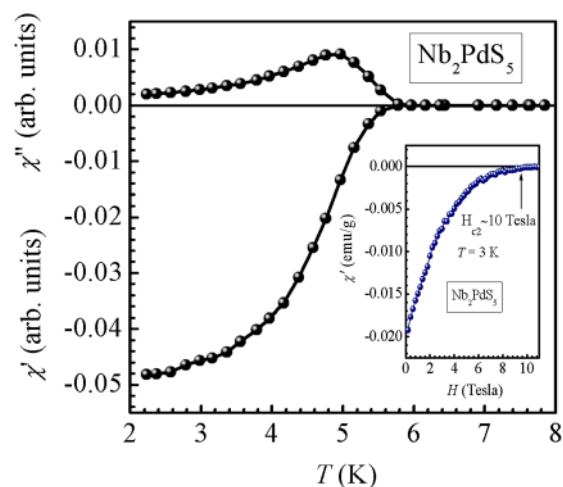


FIG. 2. AC susceptibility $\chi(T)$ behavior of the Nb_2PdS_5 sample at frequency 333 Hz and ac drive amplitude of 10 Oe, the inset shows the real part of the same in applied dc fields of up to 120 kOe.

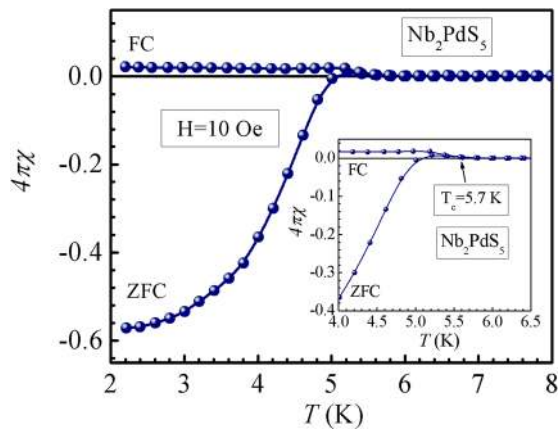


FIG. 3. Temperature variation of DC Magnetization in ZFC and FC modes for Nb_2PdS_5 compound at 10 Oe, inset shows the expanded part of the same plot indicating irreversible behavior and marking of T_c .

of 6 K. It is clear from inset of Fig. 2 that the studied Nb_2PdS_5 is bulk superconducting (diamagnetic) at 3 K in up to 100 kOe applied field. The upper critical field (H_{c2}) is above 100 kOe just 3 K below the superconducting transition temperature (T_c). This is first indication that Nb_2PdS_5 is quite robust superconductor against magnetic field. More will be discussed after magneto-transport results in the following paragraphs.

DC magnetic susceptibility of Nb_2PdS_5 sample is shown in Figure 3. The magnetization is done in both FC (Field cooled) and ZFC (Zero-field-cooled) protocol under applied magnetic field of 10 Oe. The compound shows superconducting onset, in terms of FC and ZFC bifurcation from 5.7 K. This is clear from the zoomed inset of Figure 3. There is evidence for substantial flux trapping too. The bifurcation of FC and ZFC below T_c marks the irreversible region. The shielding fraction as evidenced from ZFC diamagnetic susceptibility is quite appreciable ($\sim 58\%$). An interesting fact we found repeatedly in case of Nb_2PdS_5 superconductor is the appearance of paramagnetic meissner effect (PME) in FC magnetization. PME generally appears in heavily pinned superconductors²⁵ and could be a good prior indication of high H_{c2} .

Figure 4 depicts the resistivity versus temperature (ρ - T) measurement with and without applied magnetic field. The resistance of the sample decreases with temperature and confirms superconductivity with onset $T_c \sim 6.3$ K and T_c ($\rho = 0$) at 5.9 K. The normal state conduction is of metallic type. From the fitting of resistivity $\rho = \rho_0 + AT^2$ for low temperatures ($T_c < T < 50$ K), we obtained residual resistivity $\rho_0 = 1.27$ m Ω -cm and $A = 1.126 \times 10^{-4}$ m Ω -cm/K² values. The quadratic variation in resistivity with temperature is shown as red solid curve in Fig. 4, which is a clear indication of Fermi-liquid nature of Nb_2PdS_5 . To study the impact of applied magnetic field on superconductivity of Nb_2PdS_5 compound, the magneto-transport measurements are carried out in superconducting region, and the results are shown in inset-I of Fig. 4. With applied field of 110 kOe, the T_c ($\rho = 0$) decreases from 5.9 K (zero-field) to 2.4 K (110 kOe). As sketched in inset-II of Fig. 4, we have estimated upper critical field $H_{c2}(T)$ by using the conservative procedure of

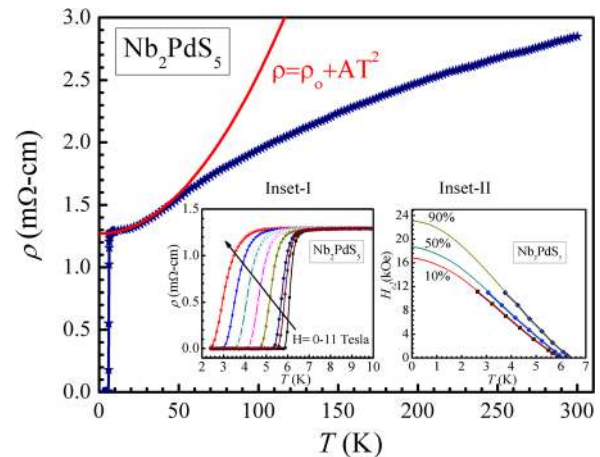


FIG. 4. Resistivity vs. temperature (ρ - T) behavior of Nb_2PdS_5 , inset-I shows the same in various applied fields of 0–110 kOe below 10 K and inset-II is the upper critical field estimated from the $\rho(T, H)$ data with 90%, 50%, and 10% ρ_n criteria.

90%, 50%, and 10% dropping of resistivity from normal state into the superconducting transition line. While the applicability of *WHH* (Werthamer-Helfand-Hohenberg) approximation can be debated in this new superconductor, a simplistic single band extrapolation leads to $H_{c2}(0)$ ($= -0.69 T_c dH_{c2}/dT|_{T_c}$) value of 240 kOe, 185 kOe, and 170 kOe with of 90%, 50%, and 10% criterion, respectively. These values match with the experimentally ascertained bulk diamagnetic response of Nb_2PdS_5 superconductor at 3 K in 100 kOe field (inset Fig. 2). The estimated values of upper critical field are close to the earlier reported values.¹² Interestingly, the $H_{c2}(0)$ value for Nb_2PdS_5 superconductor is more than the one as being expected within Pauli Paramagnetic limit of $H_{c2}(0) = 1.84T_c$ of around 110 kOe.

The relative decrement of superconductivity with applied field i.e., dT_c/dH is around 0.3 K/10 kOe from absolute T_c ($\rho = 0$) criteria. When this is compared with the best of *HTSc* cuprates (3 K/10 kOe),²⁶ Fe pnictides (1 K/10 kOe),^{6,14} pinned MgB_2 (1.5 K/10 kOe),¹⁵ or the Fe chalcogenides (0.4 K/10 kOe)^{7,8} and Chevrel phase (0.45 K/10 kOe)²⁷ compounds, one finds that Nb_2PdS_5 is the most robust superconductor against magnetic field till date.

Figure 5 shows the heat capacity (C_p) versus temperature (T) plots at different applied fields of 0, 10, 50, and 140 kOe in superconducting region i.e., 2–8 K for studied Nb_2PdS_5 superconductor. In normal state i.e., at 200 K, the value of C_p is around 180 J/mole K, see inset of Figure 5. The superconducting transition temperature (T_c) is seen clearly as a hump in C_p at around 6 K. As evident from Fig. 5, the C_p peak temperature shifts to lower temperatures with application of external field and is namely at 5.5 K, 5.2 K, and 4.2 K at 0, 10 kOe, and 50 kOe, respectively. The C_p hump and associated peak temperature is not seen down to 2 K at 140 kOe magnetic field. This shows the compound is not superconducting down to 2 K in applied field of 140 kOe.

Figure 6 shows the low temperature normal-state 140 kOe $C_p(T)$ data from 2–10 K, which is fitted to the Sommerfeld–Debye expression as $C_p(T) = \gamma T + \beta T^3 + \delta T^5$. The values of Sommerfeld constant (γ) and β are obtained

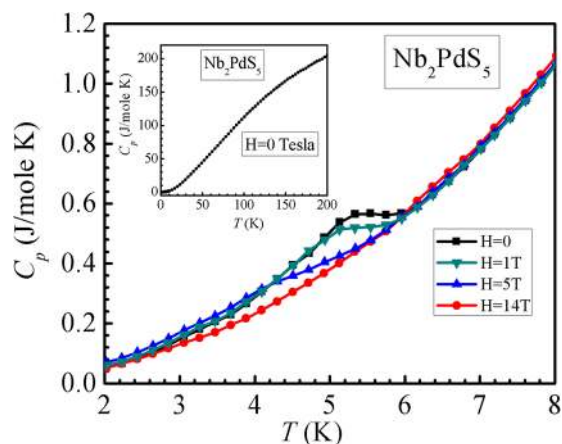


FIG. 5. Heat capacity (C_p) versus temperature plot for Nb_2PdS_5 superconductor; inset shows the same in 0, 10, 50, and 140 kOe fields in superconductivity region below 8 K.

from the fitting of the experimental data are as $\gamma = 32 \text{ mJ/mol-K}^2$, $\beta = 1.79 \text{ mJ/mol-K}^4$ and $\delta = -3.48 \times 10^{-3} \text{ mJ/mol-K}^6$. The heat capacity jump ($\Delta C = C_s - C_p$) is estimated by subtracting superconducting heat capacity (C_s) to the normal state fitted C_p and the same is shown in the inset of Fig. 6. The normalized value of jump ($\Delta C/\gamma T_c$) is ~ 0.75 , which is less than in comparison to the Bardeen–Cooper–Schrieffer (BCS) value of 1.43. As seen from inset of Fig. 6, the C_p peak exhibits multiple gap superconductivity signatures with three different T_c , with slight upturn near 2 K. The relatively higher value of $\gamma = 35 \text{ mJ/mol-K}^2$ is an indication that the Nb_2PdS_5 is a strongly coupled superconductor.²³ Worth mentioning is the fact that β and γ values change slightly, when instead of extended low T fitting of experimental C_p to normal state, the 140 kOe low T experimental data are taken as normal state. Yet, the fact remains that the normalized value of C_p jump is smaller than BCS value and the same clearly demonstrates the multi gap superconductivity. The Debye temperature is calculated by using $\Theta_D = (234zR/\beta)^{1/3}$; here, z being number of atoms per formula unit and R is the gas constant. Taking the fitted value of β (1.79 mJ/mol-K^4), the calculated value of Θ_D is 263 K.

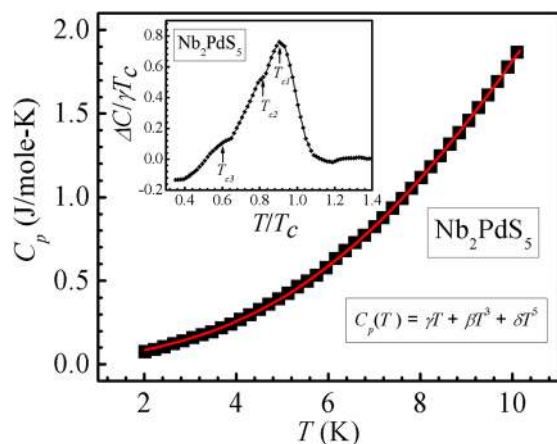


FIG. 6. Fitted (red line) and observed (filled squares) C_p versus T data for Nb_2PdS_5 at applied field of 140 kOe in low temperature region, the inset shows the electronic specific heat peak at T_c .

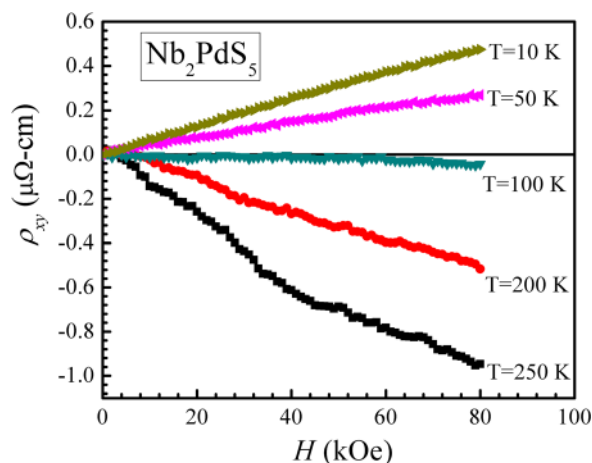


FIG. 7. Hall resistivity (ρ_{xy}) versus magnetic field plots at various temperatures of 250 K, 200 K, 100 K, 50 K, and 10 K for Nb_2PdS_5 superconductor.

In order to understand the carries contribution to transport properties in un-doped Nb_2PdS_5 , Hall resistivity (ρ_{xy}) and Hall coefficient (R_H) measurements were carried out in normal state at different temperatures. Figure 7 depicts the Hall resistivity (ρ_{xy}) results for studied Nb_2PdS_5 superconductor at various temperatures of 250 K, 200 K, 100 K, 50 K, and 10 K up to applied magnetic field of 80 kOe. The magnetic field is applied perpendicular to the current flow direction and the voltage is recorded by five probe resistivity measurement method to minimize the magneto resistance contribution. It is clear from Fig. 7 that holes dominate the transport below temperatures 100 K, whereas electrons at and above 100 K. Clearly, this indicates that the Nb_2PdS_5 exhibits a change in type of dominating charge carriers at around 100 K. To assert this behavior further, the Hall coefficient (R_H) of Nb_2PdS_5 sample is measured under three different applied magnetic fields 5 kOe, 30 kOe, and 50 kOe in the temperature range of 2 to 300 K, which is shown in Fig. 8. It can be observed from Fig. 8 that the R_H changes its sign from negative (electron type) to positive (hole type) around 190 K

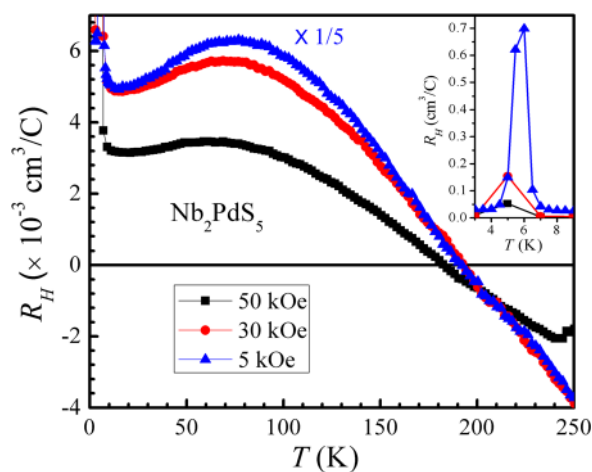


FIG. 8. Hall coefficient (R_H) versus temperature plot for Nb_2PdS_5 superconductor under applied fields of 5 kOe, 30 kOe, and 50 kOe. 5 kOe $R_H(T)$ is multiplied by 1/5 for the clarity of viewgraph. Magnified graph close to superconducting transition is shown in inset.

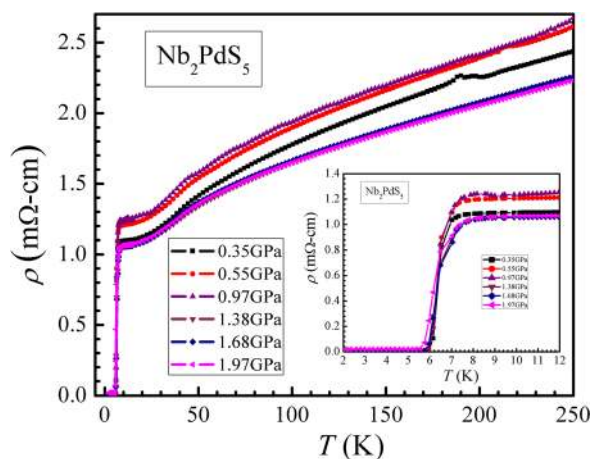


FIG. 9. Resistivity under different hydrostatic pressure (0.35–1.98 GPa) as function of temperature for Nb_2PdS_5 superconductor, inset shows the magnified view of the same close to superconducting transition.

for all the three fields just after meeting together. R_H is known to be sensitive to curvature of Fermi surface and renormalized Fermi velocity which may lead to change in the sign of Hall coefficient with temperature.²⁸ Alternatively, this behavior can be understood by compensated two band model as proposed by Rullier-Albenque *et al.* to explain transport behavior of LiFeAs .²⁹ This compensated two band transport property in normal state corroborates multiband superconductivity as claimed by heat capacity study for Nb_2PdS_5 compound. Spectroscopic investigations need to further furnish this claim. It is also observed that in normal state, the maximum of R_H (i.e., carrier concentration, n , is minimum) is at $T_{RH(\max)} \sim 80$ K even for three different magnetic fields though value of R_H differs. It is interesting to note that this temperature [$T_{RH(\max)}$] is very close to temperature at which Hall resistivity (ρ_{xy}) changes its sign from negative to positive and not at which R_H changes its sign. Hall coefficient (R_H) sharply peaked to maximum at superconducting transition as shown in the inset of Fig. 8. For the applied field of 5 kOe, $R_H = 7.01 \text{ cm}^3/\text{C}$ which is equivalent to hole concentration $n = 1/e \cdot R_H = 8.92 \times 10^{21}/\text{cm}^3$. Similar type of carrier sign change is seen in another related superconductor 2H-NbS₂.^{28,30} Interestingly, 2H-NbS₂ is a known superconductor with T_c above 6 K.^{28,30,31} This prompted us to check if the reported superconductivity of Nb_2PdS_5 could arise possibly due to minor 2H-NbS₂ phase. To exclude the possibility of 2H-NbS₂ impurity phase driven superconductivity in Nb_2PdS_5 , we synthesized the NbS₂ compound by same heat treatment of quartz vacuum encapsulation and heating of up to 850 °C. Thus obtained NbS₂ is crystallized in $R3m$ space group with a and c parameters of 3.335 Å and 17.86 Å (Ref. 32) and is not superconducting down to 2 K, plots not shown. This clearly excluded the possibility of appearance of NbS₂ impurity driven superconductivity in Nb_2PdS_5 . To further the investigation of transport properties of Nb_2PdS_5 resistivity as a function of temperature, $\rho(T)$, is measured under various hydrostatic pressures up to 1.98 GPa, which is shown in Fig. 9. There is no appreciable change on T_c as can be seen from the inset of Fig. 9. The normal state resistivity is though slightly increased for lower pressures of up to 0.97 GPa, the

same exhibits decreasing trend for 1.68 and 1.97 GPa pressures. On the other hand, we found nearly no change in T_c .

CONCLUSIONS

In conclusion, we have synthesized the new layered sulfide Nb_2PdS_5 superconductor and established its bulk superconductivity by magnetization, transport, and heat capacity measurements below 6 K, with high upper critical field outside Pauli paramagnetic limit. The C_p measurements exhibited multiple gap superconductivity signatures with three different T_c . The Sommerfeld constant (γ) and Debye temperature (Θ_D) as determined from low temperature fitting of $C_p(T)$ are 35 mJ/mole-K² and 253 K, respectively. Hall studies in conjunction to heat capacity measurements affirm the possibility of multiband superconductivity in Nb_2PdS_5 .

ACKNOWLEDGMENTS

Authors would like to thank their Director Professor R. C. Budhani for his keen interest in the present work. This work was supported by DAE-SRC outstanding investigator award scheme to work on search for new superconductors. H. Kishan thanks CSIR for providing Emeritus Scientist Fellowship.

- ¹Q. Zhang, G. Li, D. Rhodes, A. Kiswandhi, T. Besara, B. Zeng, J. Sun, T. Siegrist, M. D. Johannes, and L. Balicas, *Sci. Rep.* **3**, 1446 (2013).
- ²Y. Kamihara, T. Watanabe, M. Hirano, and H. Hosono, *J. Am. Chem. Soc.* **130**, 3296 (2008).
- ³J. G. Bednorz and K. A. Müller, *Z. Phys. B* **64**, 189 (1986).
- ⁴J. Nagamatsu, N. Nakagawa, T. Muranaka, Y. Zenitani, and J. Akimitsu, *Nature (London)* **410**, 63 (2001).
- ⁵X. H. Chen, T. Wu, G. Wu, R. H. Liu, H. Chen, and D. F. Fang, *Nature (London)* **453**, 761 (2008).
- ⁶V. P. S. Awana, R. S. Meena, A. Pal, A. Vajpayee, K. V. R. Rao, and H. Kishan, *Euro Phys. J B* **79**, 139 (2011).
- ⁷F. C. Hsu, J. Y. Luo, T. K. Chen, T. W. Huang, Y. C. Lee, Y. L. Huang, Y. Y. Chu, D. C. Yan, and M. K. Wu, *Proc. Natl. Acad. Sci. U.S.A.* **105**, 14262 (2008).
- ⁸Y. Mizuguchi, F. Tomioka, S. Tsuda, T. Yamaguchi, and Y. Takano, *Appl. Phys. Lett.* **94**, 012503 (2009).
- ⁹Y. Mizuguchi, S. Demura, K. Deguchi, Y. Takano, H. Fujihisa, Y. Gotoh, H. Izawa, and O. J. Miura, *Phys. Soc. Jpn.* **81**, 114725 (2012).
- ¹⁰V. P. S. Awana, A. Kumar, R. Jha, S. K. Singh, A. Pal, Shruti, and S. P. Patnaik, *Solid State Commun.* **157**, 21 (2013).
- ¹¹R. Jha, A. Kumar, S. K. Singh, and V. P. S. Awana, *J. Appl. Phys.* **113**, 056102 (2013).
- ¹²C. Q. Niu, J. H. Yang, Y. K. Li, B. Chen, N. Zhou, J. Chen, J. L. Jiang, B. Chen, X. X. Yang, C. Cao, J. Dai, and X. Xu, *Phys. Rev. B* **88**, 104507 (2013).
- ¹³E. Helfand and N. R. Werthamer, *Phys. Rev.* **147**, 288 (1966).
- ¹⁴A. Srivastava, A. Pal, S. Singh, C. Shekhar, H. K. Singh, V. P. S. Awana, and O. N. Srivastava, *AIP Adv.* **3**, 092113 (2013).
- ¹⁵A. Vajpayee, R. Jha, A. K. Srivastava, H. Kishan, M. Tropeano, C. Ferdeghini, and V. P. S. Awana, *Sup. Sci. Tech.* **24**, 045013 (2011).
- ¹⁶B. T. Matthias, T. Geballe, and V. Compton, *Rev. Mod. Phys.* **35**, 1 (1963).
- ¹⁷M. Wells, M. Pickus, K. Kennedy, and V. Zaccay, *Phys. Rev. Lett.* **12**, 536 (1964).
- ¹⁸T. H. Courtney, J. Reintjes, and J. Wulff, *J. Appl. Phys.* **36**, 660 (1965).
- ¹⁹B. T. Matthias, T. H. Geballe, S. Geller, and E. Corenzwit, *Phys. Rev. B* **95**, 1435 (1954).
- ²⁰G. Oya and E. J. Saur, *J. Low Temp. Phys.* **34**, 569 (1979).
- ²¹B. Chevrel, M. Sergent, and J. J. Prigent, *Solid State Chem.* **3**, 515 (1971).
- ²²Y. F. Lu, T. Takayama, A. F. Bangura, Y. Katsura, D. Hashizume, and H. Takagi, *J. Phys. Soc. Japan.* **83**, 023702 (2014).

- ²³D. J. Singh, *Phys. Rev. B* **88**, 174508 (2013).
- ²⁴H. Yu, M. Zuo, L. Zhang, S. Tan, C. Zhang, and Y. Zhang, *J. Am. Chem. Soc.* **135**, 12987 (2013).
- ²⁵W. Braunisch, N. Knauf, V. Kataev, S. Newhausen, R. Grutz, B. Roden, D. Khomskii, and D. Wohlleben, *Phys. Rev. Lett.* **68**, 1908 (1992).
- ²⁶N. P. Liyanawaduge, S. K. W. Singh, A. Kumar, R. Jha, B. S. B. Karunaratne, and V. P. S. Awana, *Sup. Sci. Tech.* **25**, 035017 (2012).
- ²⁷K. Okuda, M. Kitagawa, T. Sakakibara, and M. J. Date, *Phys. Soc. Jpn.* **48**, 2157 (1980).
- ²⁸D. V. Evtushinsky, A. A. Kordyuk, V. B. Zabolotnyy, D. S. Inosov, B. Büchner, H. Berger, L. Patthey, R. Follath, and S. V. Borisenko, *Phys. Rev. Lett.* **100**, 236402 (2008).
- ²⁹F. Rullier-Albenque, D. Colson, A. Forget, and H. Alloul, *Phys. Rev. Lett.* **109**, 187005 (2012).
- ³⁰I. Guillamón, H. Suderow, S. Vieira, L. Cario, P. Diener, and P. Rodière, *Phys. Rev. Lett.* **101**, 166407 (2008).
- ³¹J. Kacmarcik, Z. Pribulova, C. Marcenat, T. Klein, P. Rodiere, L. Cario, and P. Samuely, *Phys. Rev. B* **82**, 014518 (2010).
- ³²B. Morosin, *Acta Cryst. B* **30**, 551 (1974).